Direct Inhibition of Insulin-Like Growth Factor-I Receptor Kinase Activity by (−)−Epigallocatechin-3-Gallate Regulates Cell Transformation

Ming Li,[1] Zhiwei He,[1] Svetlana Ermakova,[1] Duo Zheng,[1] Faqing Tang,[1] Yong-Yeon Cho,[1] Feng Zhu,[1] Wei-Ya Ma,[1] Yuk Sham,[2] Evgeny A. Rogozin,[1] Ann M. Bode,[1] Ya Cao,[3] and Zigang Dong[1]

[1]Hormel Institute, University of Minnesota, Austin, Minnesota; [2]Computational Biology/Biochemistry Consultant, Supercomputing Institute, University of Minnesota, Minneapolis, Minnesota; and [3]Cancer Research Institute, Xiangya School of Medicine, Central South University, Changsha, Hunan, China

Abstract

Insulin-like growth factor-I receptor (IGF-IR) has been implicated in cancer pathophysiology. Furthermore, impairment of IGF-IR signaling in various cancer cell lines caused inhibition of the transformed phenotype as determined by the inhibition of colony formation in soft agar and the inhibition of tumor formation in athymic nude mice. Thus, the IGF-IR might be an attractive target for cancer prevention. We showed that the tea polyphenol, (−)−epigallocatechin-3-gallate (EGCG), is a small-molecule inhibitor of IGF-IR activity (IC_{50} of 14 μmol/L). EGCG abrogated anchorage-independent growth induced by IGF-IR overexpression and also prevented human breast and cervical cancer cell phenotype expression through inhibition of IGF-IR downstream signaling. Our findings are the first to show that the IGF-IR is a novel binding protein of EGCG and thus may help explain the chemopreventive effect of EGCG on cancer development. (Cancer Epidemiol Biomarkers Prev 2007;16(3):598–605)

Introduction

The insulin-like growth factor (IGF)-I receptor (IGF-IR) is a tyrosine kinase receptor that is activated by the binding of secreted growth factors, IGF-I or IGF-II. The IGF-IR is a heterotetrameric transmembrane glycoprotein with two identical α-subunits, which are responsible for ligand binding, and two identical β-subunits, which contain a juxtamembrane domain, an ATP binding pocket, an intracellular tyrosine kinase domain, and COOH terminus, and are joined by disulfide bridges (1). On ligand interaction with the IGF-IRα subunit, residues in the tyrosine kinase domain of the β-subunit are autophosphorylated. Additional phosphorylation sites adjacent to these tyrosine residues can serve as a docking site for the adaptor protein, insulin receptor substrate-1 (IRS-1), which mediates activity through the regulatory subunits of phosphatidylinositol 3-kinase. The receptor can also recruit the Src homology-2 domain containing transforming protein, leading to activation of the Ras/Raf/mitogen-activated protein kinase/extracellular signal-regulated kinase (ERK) kinase/ERK pathway (2, 3).

Most likely because of its mitogenic, antiapoptotic properties and transformation, the IGF-IR has been implicated in cancer pathophysiology (4). A broad range of human cancers exhibit IGF-IR overexpression or increases in its kinase activity. In primary prostate cancer cells, a significant up-regulation of IGF-IR mRNA and protein levels was found compared with benign prostatic epithelium (5). During progression of colorectal adenoma to carcinoma, an increase of IGF-IR staining correlated with a higher grade and stage of the tumors (6). On the other hand, targeting of IGF-IR signaling by many different approaches, including inhibition of IGF-IR expression, blocking of ligand/receptor interactions, and impairment of receptor activation caused a reversal of the transformed phenotype and induced apoptosis *in vitro* and *in vivo* (4). Both the proliferation of cells growing under anchorage-independent conditions in soft agar and cells transplanted as xenografts into mice are dramatically decreased by impairment of IGF-IR signaling (7-13). Taken together, these observations suggested that interference with IGF-IR signaling might have anticancer effects, and therefore, an inhibitor of IGF-IR kinase activity could be a potential antineoplastic agent.

Human epidemiologic and rodent carcinogenesis studies provided evidence that green tea has chemopreventive effects for a wide range of malignancies (14-20). Mechanistic studies have indicated that (−)−epigallocatechin-3-gallate (EGCG), a major component of green tea, exerts various anticancer effects, including suppression of growth factor–mediated proliferation (16), inhibition of transformation (15), and repression of angiogenesis (17, 19). Tea and tea polyphenols have shown inhibitory activity during the initiation, promotion, and progression stages of carcinogenesis (18, 20, 21). *In vitro*, tea polyphenols, especially EGCG, have been shown to cause growth inhibition and apoptosis in several human tumor cell lines, including melanoma, breast cancer, lung cancer, leukemia, and colon cancer (20). However, the molecular mechanisms underlying the anticancer effects of green tea are still not well understood.

In the present study, we showed that EGCG is a highly potent inhibitor of IGF-IR tyrosine kinase activity and malignant cell growth. Furthermore, we found that IGF-IR autophosphorylation in the presence of increasing ATP concentrations was unaltered by EGCG treatment. This report is the first to show that EGCG can block IGF-IR kinase activity and phosphorylation of its downstream targets, resulting in an inhibition of IGF-IR–mediated cell proliferation and transformation. These studies provide proof of principle for EGCG inhibition of kinase activity, which could help in explaining the preventive effect of green tea on cancer.

Received 10/23/06; revised 12/6/06; accepted 12/15/06.

Grant support: The Hormel Foundation and NIH grants CA81064 and CA88961.

The costs of publication of this article were defrayed in part by the payment of page charges. This article must therefore be hereby marked *advertisement* in accordance with 18 U.S.C. Section 1734 solely to indicate this fact.

Note: The University of Minnesota is an equal opportunity educator and an employer.

Requests for reprints: Zigang Dong, Hormel Institute, University of Minnesota, 801 16th Avenue Northeast, Austin, MN 55912. Phone: 507-437-9600; Fax: 507-437-9606. E-mail: zgdong@hi.umn.edu

doi:10.1158/1055-9965.EPI-06-0892

Materials and Methods

Reagents. EGCG (>99.7% purity) was a kind gift from Dr. Chi-Tang Ho (Rutgers University, Piscataway, NJ). For experimental purposes, EGCG was dissolved in DMSO (0.5 mmol/L) before addition to cell cultures or cell-free solutions. Antibodies against phosphorylated Akt (Ser^{473}), total Akt, phosphorylated ERKs (Tyr^{202}/Tyr^{204}), total ERKs, total IRS-1, and phosphorylated IGF-IR (Tyr^{1131}) were purchased from Cell Signaling Technology, Inc. (Beverly, MA). Active IGF-IR (Δ1-958), IGF-IRtide substrate, and antibodies against the α-subunits or the β-subunit of IGF-IR were from Upstate Biotechnology, Inc. (Charlottesville, VA). The antibody against phosphorylation of tyrosine was from Santa Cruz Biotechnology (Santa Cruz, CA). IRDye800-conjugated affinity-purified antirabbit IgG and IRDye800-conjugated affinity-purified antimouse IgG were from Rockland Biotechnology, Inc. (Lincoln, NE). Chemical reagents, including Tris, NaCl, and SDS, for molecular biology and buffer preparation were purchased from Sigma-Aldrich (St. Louis, MO). Cell culture medium and other supplements were purchased from Life Technologies, Inc. (Carlsbad, CA). CNBr-Sepharose 4B and [γ-^{32}P]ATP were from Amersham (Piscataway, NJ). G-418, protein A/G-agarose, the CellTiter 96 AQueous One Solution Cell Proliferation Assay kit, and Signal TECT Protein Tyrosine Kinase Assay System were purchased from Promega (Madison, WI). LipofectAMINE Plus reagent was from Invitrogen (Carlsbad, CA).

Construction and Mutagenesis of IGF-IR Expression Vector. The whole IGF-IR coding fragment digested with *Xba*I/*Bam*HI from the pCVN-IGF-IR plasmid, kindly provided by Dr. Renato Baserga (Thomas Jefferson University, Philadelphia, PA), was cloned into *Xba*I/*Bam*HI sites of the pcDNA3.1 (−) Zoecin vector (Promega). Two mutant IGF-IR cDNAs, in which the codons specifying lysine residue 1003 and aspargine residue 1123 were replaced with alanine, were created by PCR-assisted *in vitro* mutagenesis. For K1003A mutation, a pair of sense and antisense primers, 5′-CCAGAGTGGCCATT*GC*AACAGTGAACGAGGCCGC-3′ and 5′-GCGGCCTCGTTCACTGTT*GC*AATGGCCACTCTGG-3′, and another pair of the primers for IGF-IR D1123A, 5′-CACAGTCAAAATCGGAGCTTTTGGTATGACGCGAG-3′ and 5′-CTCGCGTCATACCAAAA*G*CTCCGATTTTGACTGTG-3′ (mutant sites are in italics), were synthesized (Sigma-Aldrich). The nucleotide substitutions were accomplished by using the QuickChange Site-Directed Mutagenesis kit (Stratagene, La Jolla, CA). The products of the reaction were digested with *Eco*RV and ligated into the pcDNA3.1-IGF-IR cDNA construct digested previously with *Eco*RV and dephosphorylated by calf intestinal phosphatase. The sequence of the whole region derived from PCR was confirmed by sequencing. Plasmids were designated as pcDNA3.1-IGF-IRK1003A and pcDNA3.1-IGF-IRD1123A.

Cell Culture and Transfection. R^- cells are IGF-IR–negative 3T3-like fibroblasts derived from mouse embryos with a targeted disruption of the *IGF-IR* gene. R^+ cells are R^- cells stably cotransfected with the plasmid pCVN-IGF-IR, expressing the wild-type human IGF-IR cDNA under the control of a SV40 promoter, and a hygromycin B–resistant plasmid (22). R^+ and R^- cells were kindly provided by Dr. Renato Baserga. The cells were cultured in monolayers in DMEM supplemented with 10% fetal bovine serum (FBS) at 37°C in a 5% CO_2, humidified incubator. R^- cells were cultured in the presence of G-418 (50 μg/mL) and R^+ cells with hygromycin B (50 μg/mL; Roche, Indianapolis, IN). The YF3 cell line was derived from NIH3T3 mouse fibroblast cells overexpressing a mutant IGF-IR, in which the cluster of three tyrosine residues at positions 1131, 1135, and 1136 was replaced by phenylalanine residues and was kindly provided by Dr. Derek LeRoith (Diabetes Branch, National Institutes of Diabetes, Digestive and Kidney Diseases, NIH, Bethesda, MD). The MCF-7 and HeLa cell lines were cultured in MEM with 2 mmol/L L-glutamine and Earle's BSS adjusted to contain 1.5 g/L sodium bicarbonate, 0.1 mmol/L nonessential amino acids, 1 mmol/L sodium pyruvate, and 10% FBS. In addition, 0.01 mg/mL bovine insulin was added to the culture medium for MCF-7 cells. R^- cells (4×10^4/mL) in 10% FBS/DMEM were seeded in 60-mm tissue culture dishes. After culturing at 37°C for 16 h, the cells were transfected with 2 μg pcDNA3.1-IGF-IR, pcDNA3.1-IGF-IRK1003A, or pcDNA3.1-IGF-IRD1123A using the LipofectAMINE Plus reagent following the manufacturer's suggested protocol.

Tyrosine Kinase Assay. The IGF-IR *in vitro* kinase assay was done at 30°C for 30 min in a 25 μL reaction mixture containing kinase buffer [50 mmol/L Tris-HCl (pH 7.5), 0.1 mmol/L EGTA, 1% 2-mercaptoethanol, 2.5 mmol/L $MnCl_2$, 0.1 mmol/L sodium orthovanadate], 200 ng of commercially available active IGF-IR, 6.25 nmol of the kinase substrate (IGF-IRtide), EGCG (1-20 μmol/L), 100 μmol/L ATP, and 1 μCi [γ-^{32}P]ATP. After boiling for 5 min, 10 μL of the samples were separated by a Criterion Precast Gel (10-20% Tris-Tricine/peptide; Bio-Rad, Hercules, CA). After electrophoresis, the gel was dried using the GelAir Cellophane Support (Bio-Rad) and then put into a cassette with a phosphor image film. The exposed film was scanned and analyzed using the Storm 840 PhosphorImage system (Molecular Dynamics, Inc. Sunnyvale, CA). For the *in vivo* IGF-IR kinase activity assay, the commercially available active IGF-IR was replaced by the immunoprecipitated product. R^+ cells were starved in 0.1% FBS/DMEM at 37°C in a 5% CO_2 incubator for 24 h followed by treatment with EGCG at various concentrations for 1 h. Cells were then stimulated with IGF-I (20 ng/mL) for 10 min and harvested with lysis buffer [50 mmol/L Tris-HCl (pH 8.0), 5 mmol/L EDTA (pH 8.0), 150 mmol/L NaCl, 0.5 mmol/L DTT, 2 μg/mL aprotinin, 2 μg/mL leupeptin, 0.5 mmol/L phenylmethylsulfonyl fluoride, 0.5% Ninidet P-40]. Protein concentration was determined by the Modified-Lowry protein assay (Bio-Rad). Samples (500 μg) were incubated with 2 μg anti–IGF-IR β-subunit overnight at 4°C. The immunocomplex was captured by adding 50 μL of washed protein A/G-agarose slurry followed by rocking the reaction mixture at room temperature for 1 h. After washing, the immunoprecipitated beads were resuspended in kinase buffer, which was used as the active IGF-IR for the above *in vitro* IGF-IR kinase assay.

Estimation of IC_{50} for EGCG Inhibition of IGF-IR Kinase Activity. The IC_{50} value for EGCG inhibition of IGF-IR kinase activity was determined by using the Signal TECT Protein Tyrosine Kinase Assay System kit following the instructions from Promega. Briefly, 25 μL of reaction buffer containing 1× protein tyrosine kinase assay buffer, 0.1 mmol/L sodium vanadate, 25 μmol/L ATP, and 0.2 μCi [γ-^{32}P]ATP with or without 60 μmol/L PRK Biosubstrate 1 were incubated at 30°C for 5 min and then 40 ng of active IGF-IR were added. After incubating at 30°C for another 60 min, 12.5 μL of termination buffer were added to stop the reaction. Samples were spotted onto membranes, and after a series of washings, radioactivity was detected in samples by scintillation counter.

***In vitro* EGCG Pull-Down Assay.** This method has been described previously (16, 23). Briefly, commercially available active IGF-IR (2 μg) or extracted proteins (500 μg) from R^+, R^-, or mutant YF3 cells were incubated with 50 μL EGCG-Sepharose 4B (or Sepharose 4B as a negative control, 50% slurry) in reaction buffer [50 mmol/L Tris (pH 7.5), 5 mmol/L EDTA, 150 mmol/L NaCl, 1 mmol/L DTT, 0.01% Ninidet P-40, 0.02 mmol/L phenylmethylsulfonyl fluoride, 4 μg/mL bovine serum albumin, 1× protease inhibitor cocktail]. After incubation

with gentle rocking overnight at 4°C, the beads were washed five times with washing buffer [50 mmol/L Tris (pH 7.5), 5 mmol/L EDTA, 150 mmol/L NaCl, 1 mmol/L DTT, 0.01% NP40, 0.02 mmol/L phenylmethylsulfonyl fluoride] and proteins bound to the beads were analyzed by immunoblotting. In addition, to detect whether EGCG affects ATP binding with the IGF-IR, an EGCG pull-down assay was used. Briefly, 2 μg of active IGF-IR (Δ1-958) were incubated with different concentrations of ATP (1, 10, and 100 μmol/L), 50 μL EGCG-Sepharose 4B, or 50 μL Sepharose 4B in reaction buffer in a final volume of 500 μL followed by rotating overnight at 4°C. After washing, proteins were detected by Western blot.

Molecular Modeling of the IGF-IR and Docking of EGCG. The crystal structures of the unactive apo (1P4O) and the activated ATP-bound IGF-IR (1K3A) were taken from the protein data bank. The possible existence of alternative binding sites was modeled within Sybl 7.0 (Tripos, Inc. Patterson, CA) using Sybl's Molcad program. The docking of EGCG was carried out using InsightII (San Diego, CA). Both protein structures were first sequence aligned and superimposed to compare structure variation. The structure of EGCG was then overlaid on the bound ATP in the ATP-bound IGF-IR binding site. The resultant docked EGCG-bound IGF-IR complex was then energy minimized.

Western Blotting. Cells were cultured to 80% confluence in 6-cm plates followed by starvation for 24 h and subsequent treatment with various concentrations of EGCG (0-20 μmol/L) for 1 h and then stimulated with 20 ng/mL IGF-I for 10 min. Cells were then rinsed with cold PBS and harvested in lysis buffer (see IGF-IR kinase activity assay). The disrupted samples were transferred into fresh 1.5-mL tubes and sonicated for 30 s and protein concentration was determined. Samples containing an equal amount of protein were loaded into each lane of a SDS-polyacrylamide gel for electrophoresis and subsequently transferred onto a polyvinylidene difluoride membrane. Phosphorylation of Akt and ERKs was selectively detected by IRDye800-conjugated affinity-purified antirabbit IgG or IRDye800-conjugated affinity-purified antimouse IgG using the Odyssey Infrared Imaging System (LI-COR Biosciences, Lincoln, NE). Nonphosphorylated levels of Akt and ERK were detected as internal controls to determine equal protein loading.

Cell Proliferation Assay. To assess cell proliferation, R^+ and R^- cells (2×10^3 per well) were seeded in 96-well tissue culture plates and cultured at 37°C in a 5% CO_2 incubator. Cellular proliferation was then estimated at 0 to 4 days using the CellTiter 96 AQueous One Solution Cell Proliferation Assay kit according to the manufacturer's instructions. The assay solution was added to each well and absorbance (492 and 690 nm as background) was read with a 96-well plate reader. Absorbance at 492 nm is directly proportional to the number of living cells. Then, to test whether EGCG had an effect on proliferation of R^+ and R^- cells, the cells (2×10^3 per well) were seeded in 96-well tissue culture plates in medium containing 10% FBS. After 24 h, the medium was changed into test medium containing different concentrations of EGCG (0, 2.5, 5, 10, or 20 μmol/L). After 72 h, 20 μL of the CellTiter 96 Aqueous Solution were added to each well. Cells were incubated for an additional 1 h and then absorbance was measured using a 96-well plate reader as above.

Anchorage-Independent Cell Transformation Assay. Anchorage-independent cell growth was measured in six-well plates. MCF-7, HeLa, R^+, or R^- cells (10^4 per mL) were exposed to EGCG (0-20 μmol/L) in 1 mL of 0.3% basal medium Eagle's agar containing 10% FBS with IGF-I (20 ng/mL). The cultures were maintained in a 37°C, 5% CO_2 incubator for 2 to 3 weeks, and the cell colonies were scored using a microscope and the ImagePro Plus computer software program (Media Cybernetics, Silver Spring, MD) as described by Colburn et al. (23). The effect of EGCG on cell transformation is presented as colony number per 10,000 seeded cells in soft agar.

Results

EGCG Binds to Active IGF-IR and Selectively Inhibits Its Kinase Activity *In vivo* and *In vitro* in a Dose-Dependent Manner. Identification of EGCG binding proteins or receptors is crucial in delineating the mechanism of the anticancer effects of EGCG. Here, by using EGCG-Sepharose 4B or Sepharose 4B as affinity columns, we found that EGCG can bind with the commercially available active IGF-IR (Δ1-958; Fig. 1A). These results confirmed that active IGF-IR bound with EGCG-Sepharose 4B but not Sepharose 4B. To assess the significance of EGCG binding with the IGF-IR, we determined whether EGCG could inhibit IGF-IR (Δ1-958) kinase activity in a cell-free system. Our data (Fig. 1B) showed that EGCG efficiently suppressed phosphorylation of the IGF-IR substrate, IGF-IRtide (Fig. 1B, *bottom*), with a IC_{50} value of 14 μmol/L (Fig. 1C), as well as its autophosphorylation (Fig. 1B, *top*). We next used cells overexpressing IGF-IR (R^+ cells) to determine the effect of EGCG on IGF-IR kinase activity. Cells were treated with EGCG for 1 h followed by stimulation with IGF-I (20 ng/mL) for 10 min. An antibody against the β-subunit of the IGF-IR was used for immunoprecipitation of IGF-IR for determining kinase activity. Results indicated that EGCG inhibited phosphorylation of the IGF-IRtide substrate in a dose-dependent manner (Fig. 1D). Overall, these results showed that EGCG can bind with active IGF-IR and inhibit IGF-IR kinase activity *in vitro* and *in vivo* in a dose-dependent manner.

To further confirm the binding results *in vivo*, an IGF-IR kinase domain mutant (Y1131F, Y1135F, and Y1136F) cell line (YF3) was obtained and compared with the R^+ cell line for binding with EGCG. Lysates prepared from R^+ and mutant YF3 cells were incubated with EGCG-Sepharose 4B or Sepharose 4B (as a negative control), and the pulled-down proteins were analyzed by Western blot. The IGF-IR from the mutant YF3 cell lysate cannot be autophosphorylated and therefore cannot react with anti–phosphor-IGF-IR (Fig. 1E, *bottom*) but can react with the antibody against the IGF-IR β-subunit of the IGF-IR (Fig. 1E, *top*). Results indicated that the YF3 lysate, containing the mutant IGF-IR, did not interact with the EGCG-Sepharose 4B affinity column, whereas the R^+ cell lysate showed a positive signal for IGF-IR binding with EGCG-Sepharose 4B (Fig. 1E).

We then determined the specificity of EGCG as an IGF-IR inhibitor by investigating its effect on the activity of other tyrosine kinases, including Abl, platelet-derived growth factor receptor α, c-Src, Bmx, and Yes. Results (Table 1) show that EGCG had no effect on the kinase activity of any of these tyrosine kinases.

EGCG Inhibits IGF-IR Downstream Signaling in Intact Cells. As indicated earlier, studies showed that, after binding with IGF-I, active IGF-IR induces activation and phosphorylation of several of its downstream signaling pathways, including IRS-1, phosphatidylinositol 3-kinase, and ERKs (2, 3). Because EGCG efficiently inhibits IGF-IR kinase activity, we determined whether EGCG also suppressed IGF-IR downstream events *in vivo*. IGF-IR expression was confirmed in R^+ and R^- cells (Fig. 2A). Then, R^+ and R^- cells were treated with increasing concentrations of EGCG (0-20 μmol/L) for 1 h followed by stimulation with IGF-I (20 ng/mL) for 10 min. An EGCG-induced dose-dependent decrease in phosphorylation of IRS-1, ERKs (Tyr^{202}/Tyr^{204}), and Akt (Ser^{473}) was observed (Fig. 2B-D, respectively) in R^+ cells compared with untreated control cells. Although R^- cells expressed ERKs and Akt

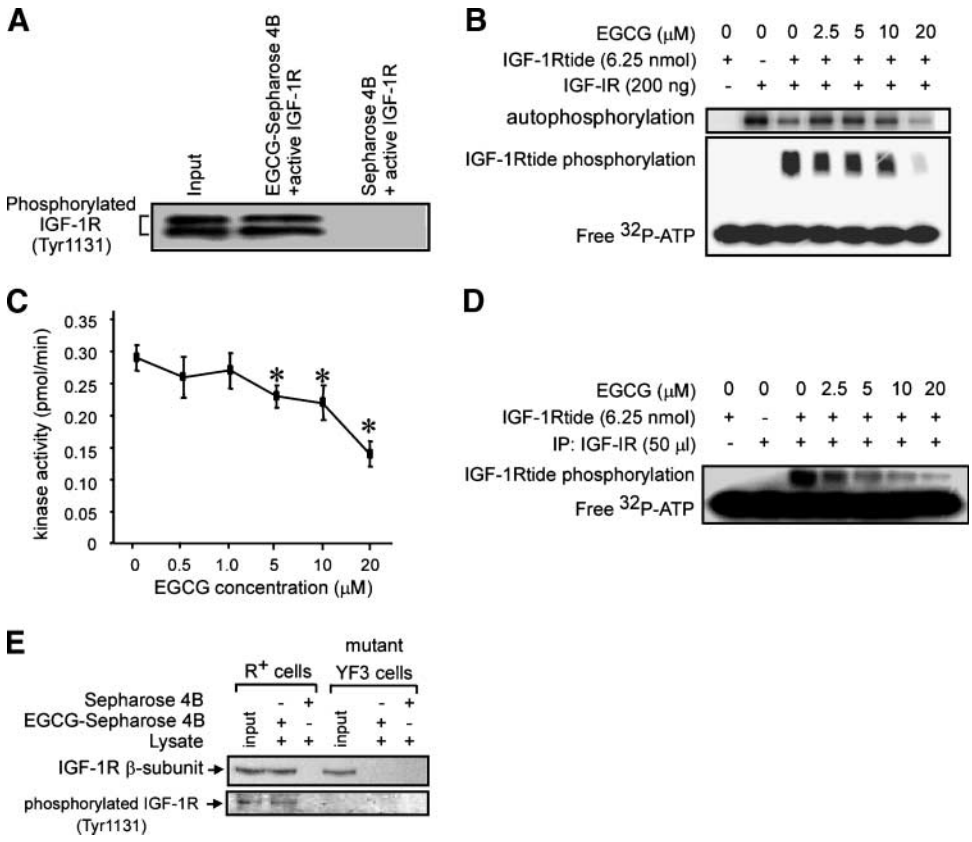

Figure 1. Effect of EGCG on IGF-IR kinase activity in a cell-free system. **A.** Immunoblot analysis of active IGF-IR (Δ1-958) following purification by an EGCG-Sepharose 4B affinity column. An EGCG-Sepharose 4B and Sepharose 4B affinity column were each incubated with commercially available, active IGF-IR (Δ1-958). After washing, the active IGF-IR/EGCG complex was confirmed by Western blot using an antibody against phosphorylated IGF-IR. **B.** Effect of EGCG on commercially available IGF-IR (Δ1-958) kinase activity. Determination of phosphorylation was carried out using a standard kinase assay in the presence of 1 μCi [γ-^{32}P]ATP with 400 ng of active IGF-IR kinase and 6.25 nmol of substrate (IGF-IRtide) in a 25 μL reaction mixture incubated with or without EGCG at the indicated concentrations for 30 min at 30°C. Autophosphorylation (*top*) and substrate phosphorylation levels (*bottom*) were detected by autoradiography. The reaction mixture without EGCG was used as a positive control (*lane 3*). Free ^{32}P was used as a loading control (*bottom*). **C.** IC_{50} for EGCG inhibition of IGF-IR kinase activity. The IC_{50} value for EGCG inhibition of IGF-IR kinase activity was determined using the Signal TECT Protein Tyrosine Kinase Assay System kit following the instructions provided by the manufacturer (see Materials and Methods). *Points,* mean of three independent experiments; *bars,* SD. *, $P < 0.05$, significant EGCG-induced decrease in kinase activity compared with untreated control. **D.** Effect of EGCG on IGF-IR kinase activity immunoprecipitated (*IP*) from R^+ cells. R^+ cells were starved for 24 h and then treated with EGCG for 1 h followed by stimulation with IGF-I (20 ng/mL) for 10 min. IGF-IR immunoprecipitated from R^+ cells was used to measure kinase activity in a cell-free system. Total phosphorylation level was determined by autoradiography. The reaction mixture without EGCG was used as a positive control (*lane 3*). **E.** Confirmation of EGCG binding with active IGF-IR *in vivo*. An EGCG-Sepharose 4B or Sepharose 4B column was incubated with lysates from R^+ or YF3 cells. After washing, the proteins binding with EGCG-Sepharose 4B or Sepharose 4B were analyzed by Western blot. *Input,* the R^+ cell lysate. YF3 lysate was used as the positive control. *Top,* first antibody against the IGF-IR β-subunit; *bottom,* first antibody against phosphorylated IGF-IR (Tyr^{1131}).

proteins, no phosphorylation of ERKs or Akt was detected (Fig. 2C and D). However, after stimulation by 10 ng/mL EGF for 5 min, ERK and Akt phosphorylation could still be detected in R^- cells (Fig. 2C and D). Next, instead of using transfected cells, we investigated whether EGCG exerted similar effects in cells that endogenously overexpress IGF-IR. Human breast cancer cells (MCF-7), which highly express IGF-IR, were treated with increasing concentrations of EGCG and stimulated with 10 ng/mL IGF-I as above. Results further indicated that EGCG had similar inhibitory effects on IGF-IR autophosphorylation (Fig. 2E) and phosphorylation of downstream targets (data not shown).

Possible Mechanism of Action of EGCG. Because part of the IGF-IR crystal structure is now available, the docking model of EGCG binding to the ATP binding pocket was extrapolated from computer modeling of the structure of the IGF-IR. The model predicted that several amino acid residues within the ATP binding pocket could contact EGCG. The calculated hydrogen bonds between EGCG and the IGF-IR are shown as green dotted lines and the participating residues include GLN977, LYS1003, MET1052, THR1053, and ASP1123 (Fig. 3A). These results suggested that EGCG might fit into the ATP binding pocket through a hydrogen-bonding network. To confirm this idea, we incubated an EGCG affinity column together with different concentrations of ATP and 2 μg of the IGF-IR. Results from immunoblotting showed that as ATP concentration increased, binding of the active IGF-IR with EGCG-Sepharose 4B decreased in a dose-dependent manner, which suggested that EGCG decreased ATP binding with the IGF-IR (Fig. 3B). Furthermore, the computer modeling data suggested that K1003 and D1123 in the ATP binding pocket of the IGF-IR are the more important amino acids for EGCG binding by supplying hydrogen bonds. Therefore, mutant (K1003A and D1123A) IGF-IR plasmids were generated and

transfected into R^- cells. These membrane proteins were expressed and extracted from transfected cells and then incubated with the EGCG affinity column. Protein binding was analyzed by Western blot and data indicated that mutation at either LYS1003Ala or ASP1123Ala greatly decreased the binding of the IGF-IR with EGCG (Fig. 3C). The residues analyzed are within the ATP binding pocket of the IGF-IR and the mutant K1003A or D1123A decreased binding between EGCG and the IGF-IR. The overall information thus far suggested that EGCG can compete with ATP in the ATP binding pocket of the IGF-IR resulting in the inhibition IGF-IR kinase activity and cell growth.

EGCG Inhibits Cell Proliferation and Anchorage-Independent Cell Transformation. The IGF-IR has been reported to have an important influence on cell proliferation. Thus, to determine the effect of EGCG on the role of IGF-IR in cell growth, we examined proliferation in R^+ and R^- with and without EGCG treatment. Results indicated that R^+ cells grew significantly ($P < 0.05$) more rapidly than cells lacking IGF-IR expression (R^- cells), over a period of 5 days (Fig. 4A). Furthermore, when cells were treated with increasing concentrations of EGCG for 72 h, proliferation was significantly inhibited by EGCG in R^+ cells but unaffected in R^- cells (Fig. 4B). Similar results were also found in IGF-IR–overexpressing MCF-7 and HeLa cells (data not shown). These results strongly supported the idea that the IGF-IR serves as a critical promoter of tumor cell proliferation, and EGCG binding with the IGF-IR results in a negative regulation of cancer cell growth.

To determine the role of EGCG in cell transformation induced by IGF-I, we used the anchorage-independent cell transformation assay. R^- cells, which have a disruption of *IGF-IR* gene expression, cannot be transformed by oncogenes unless IGF-IR expression is reintroduced (22). R^+ cells were stimulated with IGF-I and treated with increasing concentrations of EGCG. Results indicated that compared with untreated control cells, the colony numbers were greatly decreased in cells treated with EGCG (Fig. 4C and D), strongly suggesting that EGCG can suppress malignant cell transformation mediated by the IGF-IR. We then determined whether this inhibition occurred in other tumor cell lines that overexpress this receptor. As expected, EGCG inhibited phenotype expression of the breast carcinoma cell line, MCF-7 (Fig. 4E), and the cervical carcinoma cell line, HeLa (Fig. 4F), as well as anchorage-independent growth of mouse fibroblasts with ectopic overexpression of human IGF-IR (R^+ cells; Fig. 4C and D). This agrees well with data showing that EGCG caused a significantly reduced IGF-IR phosphorylation in the MCF-7 cell line (Fig. 2E).

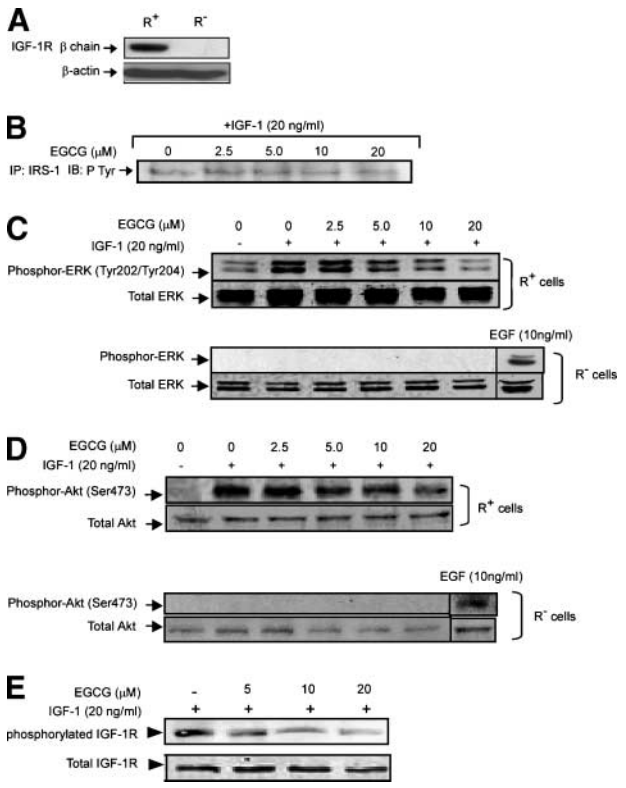

Figure 2. Effect of EGCG on IGF-IR–induced phosphorylation of downstream kinases. R^+ and R^- cells were starved for 24 h followed by incubation for 1 h with EGCG at various concentrations (0, 2.5, 5, 10, or 20 μmol/L). After stimulation with 20 ng/mL IGF-I for 10 min, cells were collected and sonicated for 30 s and protein concentration was determined. After adding 3× SDS sample buffer and heating for 5 min, 30 μg of protein were analyzed by Western blot. Equal protein loading was confirmed by detecting the respective nonphosphorylated protein on the same membrane. Data are representative of three independent experiments. **A.** Confirmation of IGF-IR expression in R^+ and R^- cells. **B.** Effect of EGCG on phosphorylation of IRS-1 in R^+ cells. **C.** Effect of EGCG on phosphorylation of ERK in R^+ and R^- cells. *Last lane* (*bottom*), the effect of EGF (10 ng/mL) on phosphorylation of ERK in R^- cells. **D.** Effect of EGCG on phosphorylation of Akt in R^+ and R^- cells. *Last lane* (*bottom*), the effect of EGF (10 ng/mL) on phosphorylation of Akt in R^- cells. **E.** Effect of EGCG on autophosphorylation of IGF-IR in MCF-7 cells. MCF-7 cells were starved for 24 h followed by stimulation with 20 ng/mL IGF-I for 10 min. The cell lysate was harvested and 30 μg of protein were analyzed by 8% SDS-PAGE and immunoblotting.

Discussion

The biological outcomes of IGF-IR activation include cell proliferation, mitogenesis, cell survival, neoplastic transformation, and metastasis (22, 24, 25). IGF-IR overexpression or its constitutively high kinase activity is associated with various cancers (25). The fact that the IGF-IR is not absolutely required for normal growth but plays an essential role in cells grown under anchorage-independent conditions or *in vivo* in transplanted tumors makes it an attractive target for cancer therapy.

Table 1. Effect of EGCG on activity of various tyrosine kinases

Tyrosine kinase	Kinase activity (% of control)
IGF-IR	77
Abl	114
PDGFRα	108
c-Src	137
Bmx	121
Yes	97

Abbreviation: PDGFRα, platelet-derived growth factor receptor α.

The most advanced strategies to block IGF-IR are those involving small inhibitors of the IGF-IR tyrosine kinase activity. In this report, we found that EGCG, the major component of green tea, inhibits IGF-IR kinase activity *in vitro* (IC_{50} of 14 μmol/L) and *in vivo* dose dependently. As expected, phosphorylation of the IRS-1, which is a substrate of the IGF-IR tyrosine kinase, was reduced by exposure to EGCG. Therefore, EGCG could effectively inhibit the IGF-IR–mediated signaling pathway, resulting in suppression of cell proliferation and transformation.

Overexpression of the IGF-IR is sufficient to transform immortalized mouse fibroblasts, as assayed by survival and

growth in soft agar and the formation of tumors in nude mice (22, 26). On the other hand, fibroblasts genetically deficient for the *IGF-IR* gene are resistant to transformation by oncoproteins, such as the SV40 T antigen, c-Src, Ras, the platelet-derived growth factor receptor, or the epidermal growth factor receptor (22, 27, 28). R^- cells, which do not express the IGF-IR, cannot form colonies in soft agar but if the *IGF-IR* gene is reintroduced, then these cells regain the ability to form colonies. In our study, the tea polyphenol, EGCG, was found to fulfill a key characteristic expected from an IGF-IR inhibitor. Notably, it effectively inhibited the survival function ascribed to IGF signaling and prevented the ability of cells overexpressing the IGF-IR to grow in an anchorage-independent manner when stimulated by IGF-I. As expected, the inhibition of

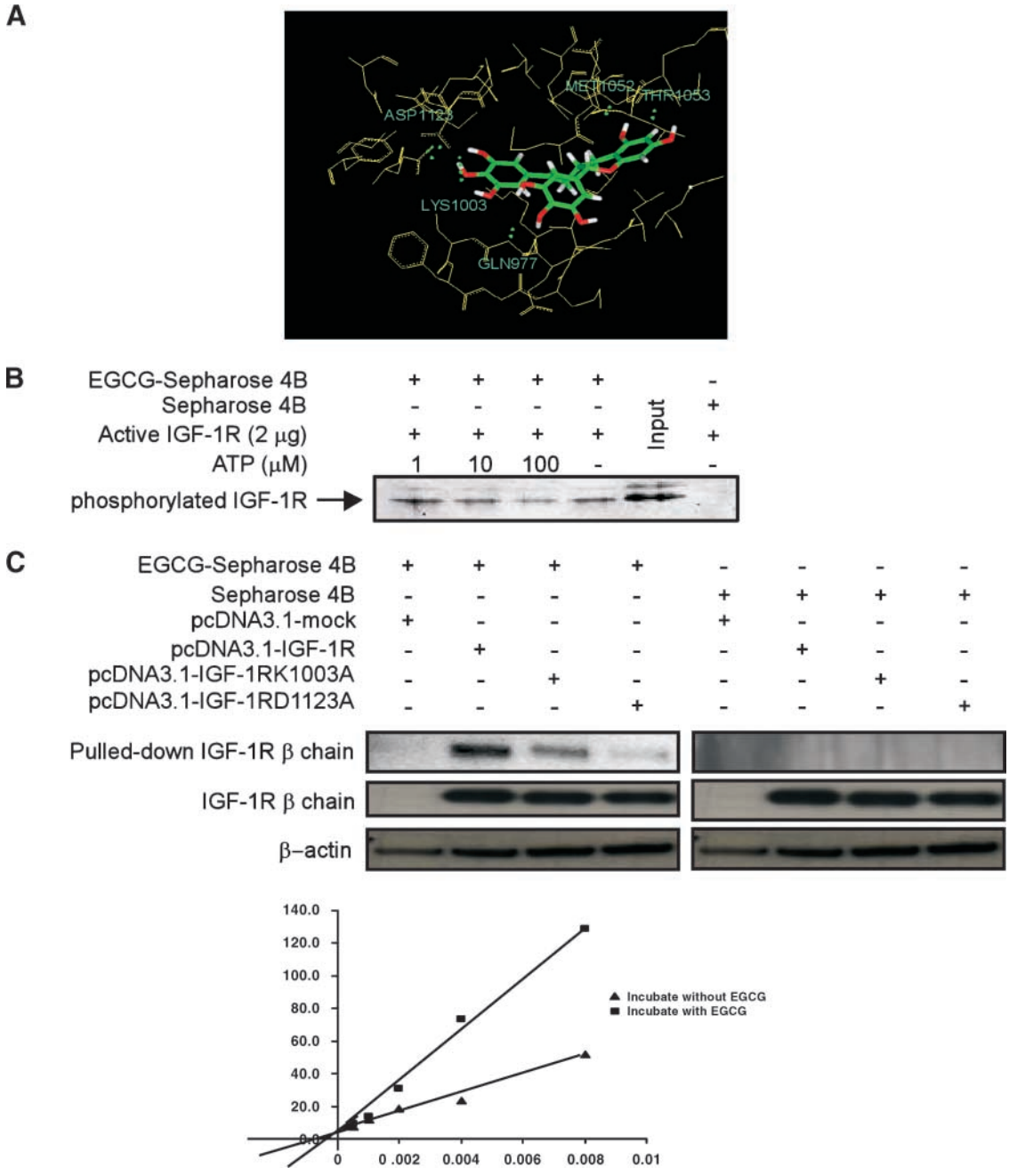

Figure 3. Comparison of the IGF-IR binding site for EGCG and ATP. **A.** Molecular modeling of IGF-IR and docking of EGCG. The binding pocket was identified from the IGF-IR crystal structure. Hydrogen bonds between EGCG and IGF-IR were calculated (*green dotted lines*). The participating residues include GLN977, LYS1003, MET1052, THR1053, and ASP1123. **B.** EGCG decreases ATP binding with IGF-IR. Active IGF-IR (Δ1-958; 2 μg) was incubated with different concentrations (0, 1, 10, and 100 μmol/L) of ATP and 50 μL EGCG-Sepharose 4B or 50 μL of Sepharose 4B (as a negative control) in reaction buffer in a final volume of 500 μL. The mixtures were incubated with shaking overnight at 4°C. After washing, the pulled-down proteins were analyzed by Western blot. **C.** EGCG binds weakly with mutant IGF-IR. R^- cells were transfected with pcDNA3.1-mock, pcDNA3.1-IGF-IR, pcDNA3.1-K1003A, or pcDNA3.1-D1123A. After stimulation with IGF-I (20 ng/mL), the membrane proteins were extracted and then incubated with EGCG-Sepharose 4B or Sepharose 4B. The binding proteins were detected by an antibody against the IGF-IR β-subunit. *Top,* the Western blot result of the proteins pulled down by EGCG Sepharose 4B or Sepharose 4B; *middle,* the expression of IGF-IR in the transfected R^- cells. β-Actin served as a loading control (*bottom*).

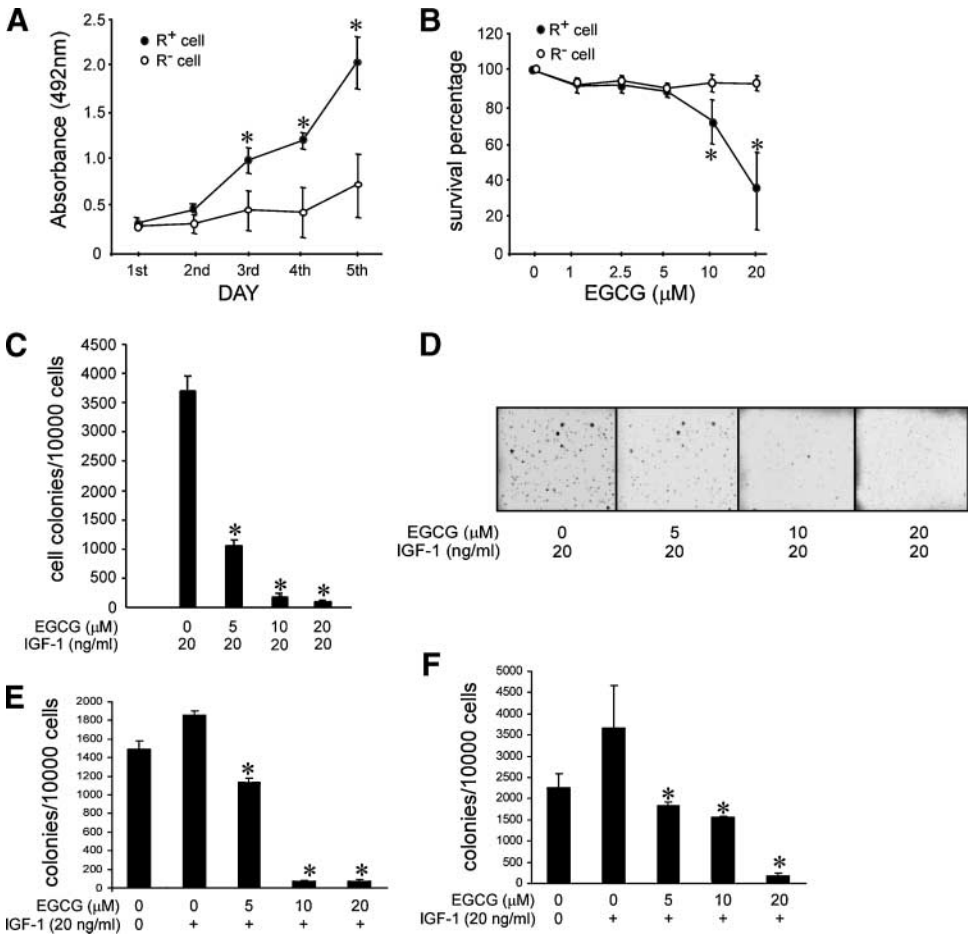

Figure 4. Effect of EGCG on IGF-I–stimulated cellular proliferation. **A.** R^+ and R^- cells (2×10^3 per well) were cultured in DMEM/FBS at 37°C in a 5% CO_2 incubator in 96-well plates. Absorbance values were determined at culture days 1, 2, 3, 4, and 5. *Points,* mean of three independent experiments; *bars,* SD. *, $P < 0.05$, significantly greater absorbance value for R^+ cells compared with R^- cells. **B.** R^+ and R^- cells (2×10^3 per well) were plated in 96-well plates and maintained for 3 d in DMEM/FBS in the presence of the indicated concentrations of EGCG. On the 3rd day, 20 μL of the CellTiter 96 AQueous One Solution were added and cells were incubated for another 1 h. Then, absorbance (492 and 690 nm as background) was measured using a 96-well plate reader. *Points,* mean of three separate wells from three independent experiments; *bars,* SD. *, $P < 0.05$, significant EGCG-induced decrease in viability of R^+ cells compared with R^- cells. **C.** Effect of EGCG on R^+ cell transformation. R^+ cells were subjected to an anchorage-independent cell transformation assay (soft agar assay) in the presence of IGF-I and various concentrations of EGCG. R^+ cells were exposed to IGF-I (20 ng/mL) in 1 mL of 0.3% basal medium Eagle's agar containing 10% FBS. The cultures were maintained in a 37°C, 5% CO_2 incubator for 3 wks, and then colonies were counted using a microscope and the ImagePro Plus computer software program. *Columns,* mean of values obtained from triplicate experiments; *bars,* SD. *, $P < 0.05$, significant EGCG-induced decrease in colony formation compared with the respective untreated control. **D.** Photographic representation of the effect of EGCG on IGF-I–induced cell transformation. **E.** Effect of EGCG on HeLa cell transformation. **F.** Effect of EGCG on MCF-7 cell transformation. *Columns,* means of values obtained from triplicate experiments; *bars,* SD (**E** and **F**). *, $P < 0.05$, significant EGCG-induced decrease in colony formation compared with the respective untreated control (**E** and **F**).

IGF-IR by EGCG also occurred in other malignant cell lines of various origins, including MCF-7 and HeLa cells, which highly express the IGF-IR. Importantly, events occurred at concentrations of EGCG that are consistent with its capacity to inhibit IGF-IR kinase activity.

Our findings are further supported by studies in the transgenic mouse prostate adenocarcinoma model (TRAMP). The IGF system contains ligands (IGF-I and IGF-II), the IGF-IR, and IGF binding proteins, especially IGF binding protein-3, which negatively controls IGF-IR activity (29). Investigators observed that serum IGF-I levels were inhibited as IGF binding protein-3 levels increased in TRAMP mice fed with green tea polyphenols (30). These changes were accompanied by inhibition of downstream signaling cascades that involve both phosphatidylinositol 3-kinase/Akt and the mitogen-activated protein kinases (30). Results suggested that the IGF/IGF binding protein-3 pathway is a potential target for green tea polyphenol–mediated inhibition of prostate cancer progression in the TRAMP mouse model (30). This work is supported by transcriptome profiling studies in Nrf2 null mice where IGF-IR was found to be strongly inhibited in both liver and small intestine by EGCG (31). Shimizu et al. (32) reported that EGCG inhibited IGF-IR activation in colon cancer cells, but no significant changes were observed in the levels of the IGF-IR proteins, which suggested that EGCG specifically suppressed activation of the IGF-IR, but did not down-regulate the total expression of these proteins (32). On the other hand, the later data further support our finding that EGCG can interact with active IGF-IR. Overall, our data clearly showed that EGCG directly inhibited IGF-IR kinase activity by competing with ATP to bind with active IGF-IR resulting in suppression of downstream signaling pathways.

Inhibition of tyrosine kinase activity could be accomplished by either blocking the ATP binding site or the substrate

binding sites in the kinase domain of the kinase. The ligand-receptor interaction results in phosphorylation of tyrosine residues in the IGF-IR tyrosine kinase domain (amino acids 973-1229) of the β-subunit. The crystal structure of the inactive and active kinase domain of the IGF-IR has provided a molecular model of the IGF-IR catalytic activity (33). In an unstimulated state, the activation loop (a-loop) containing the critical tyrosine residues 1131,1135, and 1136 behaves as a pseudosubstrate that blocks the active site resulting in preventing substrate access and occluding the ATP binding site as well. After ligand binding, the three tyrosines of the a-loop are transphosphorylated by the dimeric subunit partner. Phosphorylation of Tyr^{1135} and Tyr^{1131} destabilizes the autoinhibitory conformation of the a-loop, whereas phosphorylation of Tyr^{1136} stabilizes its catalytically optimized conformation. These changes in the a-loop conformation allow substrate and ATP access, subsequently activating downstream signaling (2, 33). When we replaced the charged hydrophilic LYS and ASP with hydrophobic ALA, the binding between EGCG and IGF-IR became weaker (Fig. 3C). In addition, using an EGCG affinity column and immunoblotting, EGCG was shown to effectively decrease ATP binding with the IGF-IR (Fig. 3B). These data strongly imply that EGCG competes with ATP binding resulting in inhibition of IGF-IR activity.

Green tea catechins, including EGCG, (−)−epigallocatechin, (−)−epicatechin gallate, and (−)−epicatechin, exhibit a range of biological activities (21). EGCG has been the most extensively studied because of its relatively high abundance and strong epidemiologic evidence supporting its antitumor activity (19, 21). Preclinical data about EGCG is promising for cancer prevention (34). A recent study has shown that EGCG inhibited focal adhesion kinase activity (35, 36) and blocked the kinase activation of the epidermal growth factor receptor/HER2 and platelet-derived growth factor receptor (15, 37). However, the site of action or mechanism by which EGCG acts as an inhibitor of these kinases is poorly understood. Nutritional or dietary factors, such as green tea, have attracted a great deal of interest because of their perceived ability to act as highly effective chemopreventive agents. EGCG, the major component of green tea, has some advantages over other blocking strategies because it seems to be nontoxic even when administered over a relatively long period. The data presented here are the first to show that EGCG inhibits cell proliferation and transformation by binding with active IGF-IR by competing with ATP, resulting in a prevention of IGF-IR downstream signaling, which may help explain the chemopreventive effect of EGCG on cancer.

References

1. Hernandez-Sanchez C, Blakesley V, Kalebic T, Helman L, LeRoith D. The role of the tyrosine kinase domain of the insulin-like growth factor-I receptor in intracellular signaling, cellular proliferation, and tumorigenesis. J Biol Chem 1995;270:29176–81.
2. Larsson O, Girnita A, Girnita L. Role of insulin-like growth factor 1 receptor signalling in cancer. Br J Cancer 2005;92:2097–101.
3. Pollak MN, Schernhammer ES, Hankinson SE. Insulin-like growth factors and neoplasia. Nat Rev Cancer 2004;4:505–18.
4. Bahr C, Groner B. The insulin like growth factor-1 receptor (IGF-1R) as a drug target: novel approaches to cancer therapy. Growth Horm IGF Res 2004;14:287–95.
5. Hellawell GO, Turner GD, Davies DR, Poulsom R, Brewster SF, Macaulay VM. Expression of the type 1 insulin-like growth factor receptor is up-regulated in primary prostate cancer and commonly persists in metastatic disease. Cancer Res 2002;62:2942–50.
6. Hakam A, Yeatman TJ, Lu L, et al. Expression of insulin-like growth factor-1 receptor in human colorectal cancer. Hum Pathol 1999;30:1128–33.
7. Li S, Ferber A, Miura M, Baserga R. Mitogenicity and transforming activity of the insulin-like growth factor-I receptor with mutations in the tyrosine kinase domain. J Biol Chem 1994;269:32558–64.
8. Mitsiades CS, Mitsiades NS, McMullan CJ, et al. Inhibition of the insulin-like growth factor receptor-1 tyrosine kinase activity as a therapeutic strategy for multiple myeloma, other hematologic malignancies, and solid tumors. Cancer Cell 2004;5:221–30.
9. Nakamura K, Hongo A, Kodama J, Miyagi Y, Yoshinouchi M, Kudo T. Down-regulation of the insulin-like growth factor I receptor by antisense RNA can reverse the transformed phenotype of human cervical cancer cell lines. Cancer Res 2000;60:760–5.
10. Reiss K, D'Ambrosio C, Tu X, Tu C, Baserga R. Inhibition of tumor growth by a dominant negative mutant of the insulin-like growth factor I receptor with a bystander effect. Clin Cancer Res 1998;4:2647–55.
11. Rininsland F, Johnson TR, Chernicky CL, Schulze E, Burfeind P, Ilan J. Suppression of insulin-like growth factor type I receptor by a triple-helix strategy inhibits IGF-I transcription and tumorigenic potential of rat C6 glioblastoma cells. Proc Natl Acad Sci U S A 1997;94:5854–9.
12. Sachdev D, Li SL, Hartell JS, Fujita-Yamaguchi Y, Miller JS, Yee D. A chimeric humanized single-chain antibody against the type I insulin-like growth factor (IGF) receptor renders breast cancer cells refractory to the mitogenic effects of IGF-I. Cancer Res 2003;63:627–35.
13. Hongo A, Yumet G, Resnicoff M, Romano G, O'Connor R, Baserga R. Inhibition of tumorigenesis and induction of apoptosis in human tumor cells by the stable expression of a myristylated COOH terminus of the insulin-like growth factor I receptor. Cancer Res 1998;58:2477–84.
14. Muto S, Yokoi T, Gondo Y, et al. Inhibition of benzo[*a*]pyrene-induced mutagenesis by (−)−epigallocatechin gallate in the lung of rpsL transgenic mice. Carcinogenesis 1999;20:421–4.
15. Sachinidis A, Seul C, Seewald S, Ahn H, Ko Y, Vetter H. Green tea compounds inhibit tyrosine phosphorylation of PDGFβ-receptor and transformation of A172 human glioblastoma. FEBS Lett 2000;471:51–5.
16. Ermakova S, Choi BY, Choi HS, Kang BS, Bode AM, Dong Z. The intermediate filament protein vimentin is a new target for epigallocatechin gallate. J Biol Chem 2005;280:16882–90.
17. Cao Y, Cao R. Angiogenesis inhibited by drinking tea. Nature 1999;398:381–1.
18. Bode AM, Dong Z. Targeting signal transduction pathways by chemopreventive agents. Mutat Res 2004;555:33–51.
19. Jung YD, Ellis LM. Inhibition of tumour invasion and angiogenesis by epigallocatechin gallate (EGCG), a major component of green tea. Int J Exp Pathol 2001;82:309–16.
20. Lambert JD, Yang CS. Cancer chemopreventive activity and bioavailability of tea and tea polyphenols. Mutat Res 2003;523–4:201–8.
21. Mukhtar H, Ahmad N. Tea polyphenols: prevention of cancer and optimizing health. Am J Clin Nutr 2000;71:1698–702S; discussion 703-4S.
22. Coppola D, Ferber A, Miura M, et al. A functional insulin-like growth factor I receptor is required for the mitogenic and transforming activities of the epidermal growth factor receptor. Mol Cell Biol 1994;14:4588–95.
23. Colburn NH, Wendel EJ, Abruzzo G. Dissociation of mitogenesis and late-stage promotion of tumor cell phenotype by phorbol esters: mitogen-resistant variants are sensitive to promotion. Proc Natl Acad Sci U S A 1981;78:6912–6.
24. Baserga R, Hongo A, Rubini M, Prisco M, Valentinis B. The IGF-I receptor in cell growth, transformation, and apoptosis. Biochim Biophys Acta 1997;1332:F105–26.
25. LeRoith D, Roberts CT, Jr. The insulin-like growth factor system and cancer. Cancer Lett 2003;195:127–37.
26. Kaleko M, Rutter WJ, Miller AD. Overexpression of the human insulinlike growth factor I receptor promotes ligand-dependent neoplastic transformation. Mol Cell Biol 1990;10:464–73.
27. Sell C, Rubini M, Rubin R, Liu JP, Efstratiadis A, Baserga R. Simian virus 40 large tumor antigen is unable to transform mouse embryonic fibroblasts lacking type 1 insulin-like growth factor receptor. Proc Natl Acad Sci U S A 1993;90:11217–21.
28. Sell C, Dumenil G, Deveaud C, et al. Effect of a null mutation of the insulin-like growth factor I receptor gene on growth and transformation of mouse embryo fibroblasts. Mol Cell Biol 1994;14:3604–12.
29. Rajaram S, Baylink DJ, Mohan S. Insulin-like growth factor-binding proteins in serum and other biological fluids: regulation and functions. Endocr Rev 1997;18:801–31.
30. Adhami VM, Siddiqui IA, Ahmad N, Gupta S, Mukhtar H. Oral consumption of green tea polyphenols inhibits insulin-like growth factor-I-induced signaling in an autochthonous mouse model of prostate cancer. Cancer Res 2004;64:8715–22.
31. Shen G, Xu C, Hu R, et al. Comparison of (−)−epigallocatechin-3-gallate elicited liver and small intestine gene expression profiles between C57BL/6J mice and C57BL/6J/Nrf2 (−/−) mice. Pharm Res 2005;22:1805–20.
32. Shimizu M, Deguchi A, Hara Y, Moriwaki H, Weinstein IB. EGCG inhibits activation of the insulin-like growth factor-1 receptor in human colon cancer cells. Biochem Biophys Res Commun 2005;334:947–53.
33. Favelyukis S, Till JH, Hubbard SR, Miller WT. Structure and autoregulation of the insulin-like growth factor 1 receptor kinase. Nat Struct Biol 2001;8:1058–63.
34. Moyers SB, Kumar NB. Green tea polyphenols and cancer chemoprevention: multiple mechanisms and endpoints for phase II trials. Nutr Rev 2004;62:204–11.
35. Liu JD, Chen SH, Lin CL, Tsai SH, Liang YC. Inhibition of melanoma growth and metastasis by combination with (−)−epigallocatechin-3-gallate and dacarbazine in mice. J Cell Biochem 2001;83:631–42.
36. Suzuki Y, Isemura M. Inhibitory effect of epigallocatechin gallate on adhesion of murine melanoma cells to laminin. Cancer Lett 2001;173:15–20.
37. Masuda M, Suzui M, Lim JT, Weinstein IB. Epigallocatechin-3-gallate inhibits activation of HER-2/*neu* and downstream signaling pathways in human head and neck and breast carcinoma cells. Clin Cancer Res 2003;9:3486–91.